

 Open access • Posted Content • DOI:10.1101/2020.12.18.423056

TFMLAB: a MATLAB toolbox for 4D traction force microscopy — [Source link](#)

Jorge Barrasa Fano, Apeksha Shapeti, Alvaro Jorge-Peñas, Mojtaba Barzegari ...+2 more authors

Institutions: Katholieke Universiteit Leuven, University of Seville

Published on: 19 Dec 2020 - bioRxiv (Cold Spring Harbor Laboratory)

Topics: Traction force microscopy

Related papers:

- [TFMLAB: A MATLAB toolbox for 4D traction force microscopy](#)
- [Software package for off-axis digital holographic microscopy imaging processing](#)
- [A visualization and segmentation toolbox for electron microscopy.](#)
- [μDIC: An open-source toolkit for digital image correlation](#)
- [From biochemical reaction networks to 3D dynamics in the cell: The ZigCell3D modeling, simulation and visualisation framework](#)

Share this paper:    

View more about this paper here: <https://typeset.io/papers/tfmlab-a-matlab-toolbox-for-4d-traction-force-microscopy-2ru4nw99v6>

1 TFMLAB: a MATLAB toolbox for 4D traction force microscopy

2

3 Jorge Barrasa-Fano¹: jorge.barrasafano@kuleuven.be

4 Apeksha Shapeti¹: apeksha.shapeti@kuleuven.be

5 Álvaro Jorge-Peñas¹: alvarojorgep@gmail.com

6 Mojtaba Barzegari¹: mojtaba.barzegari@kuleuven.be

7 José Antonio Sanz-Herrera²: jsanz@us.es

8 Hans Van Oosterwyck^{1,3*}: hans.vanoosterwyck@kuleuven.be

9

10 *Corresponding author

11 ¹Department of Mechanical Engineering, Biomechanics section, KU Leuven, Belgium

12 ²Escuela Técnica Superior de Ingeniería, Universidad de Sevilla, Spain

13 ³Prometheus, Division of Skeletal Tissue Engineering, KU Leuven, Leuven, Belgium

14

15 **Abstract.**

16 *We present TFMLAB, a MATLAB software package for 4D (x;y;z;t) Traction Force Microscopy (TFM). While various*
17 *TFM computational workflows are available in the literature, open-source programs that are easy to use by*
18 *researchers with limited technical experience and that can analyze 4D in vitro systems do not exist. TFMLAB*
19 *integrates all the computational steps to compute active cellular forces from confocal microscopy images, including*
20 *image processing, cell segmentation, image alignment, matrix displacement measurement and force recovery.*
21 *Moreover, TFMLAB eases usability by means of interactive graphical user interfaces. This work describes the*
22 *package's functionalities and analyses its performance on a real TFM case.*

23

24 **Keywords:**

25 *Traction force microscopy; cell mechanics; Image processing; Finite element method*

26

27 **1. Motivation and Significance**

28 Mechanobiology, the study of interactions between mechanical signals and biological responses, has
29 substantially grown over the last 20 years. The importance of mechanical forces in driving cell behavior is
30 now widely recognized in the literature [1]–[4]. Meanwhile, Traction Force Microscopy (TFM) has become
31 the preferred methodology to quantify forces at the cell-matrix interface. Typically, synthetic or natural
32 hydrogels mixed with cells and fiducial markers are imaged by means of optical microscopy before
33 (stressed state) and after (relaxed state) cell relaxation. Image processing algorithms measure cellular
34 force-induced deformations on the extracellular matrix (ECM) by tracking the movement of fiducial
35 markers between these two states. Finally, cell forces are retrieved by applying mechanical models that
36 relate forces to deformations. The reader is referred to excellent reviews in the field for more details [3],
37 [5], [6].

38 TFM has traditionally been applied to study cell mechanics in 2D in vitro cultures where cells are seeded
39 on top of a substrate [7]–[9]. Several open-source MATLAB software packages used in 2D (i.e. 2D
40 displacement and force calculation for 2D cell culture) and 2.5D TFM (i.e. 3D displacement and force
41 calculation for 2D cell culture) are available: displacement measurement algorithms such as Particle Image
42 Velocimetry (PIV) [10] and Particle Tracking (PT) [11], or regularization techniques for force recovery [12].
43 Moreover, “all-in-one” packages such as an ImageJ plugins [13] or the contributions by the groups of
44 Franck [14], Dufrense [15], Sabass [16] or Danuser [17] have brought complex TFM computations closer
45 to experimentalists. Current challenges lie in making TFM available for physiologically more relevant
46 experiments in 3D (cells fully embedded in a hydrogel) and incorporating time dependency (4D). Unlike
47 for 2D TFM, the availability of 3D TFM open-source tools is scarce. Some groups that are currently
48 publishing 3D TFM studies do not provide source codes [18]–[21]. Others, provide source codes but lack
49 force calculation functionalities [22]. An exception are the open source contributions of Fabry’s group.
50 They developed *SAENO* [23], the first open source 3D TFM solver for nonlinear, fibrillary materials, like
51 collagen and fibrin. While it remains a unique contribution to the field, we hereby address two limitations
52 regarding its usability by researchers with limited technical experience. First, the software does not
53 provide feedback of intermediate steps involved in the calculations (such as image filtering or shift
54 correction), which requires higher technical expertise from users to select the optimal input parameters
55 for each sample [24]. Second, while the signal to noise ratio of the images heavily depend, among others,
56 on the type of microscope or the hydrogel used, *SAENO* does not allow to adjust image processing
57 operations to new data as they are hidden from the user. More recently, they published *jointforces*, an
58 open source Python package [25]. While they applied it for data from a 3D in vitro model of a tumor
59 spheroid, the software only calculates 2D forces at the equatorial plane of the spheroid.

60 With *TFMLAB*, we provide an “all-in-one” open source 4D (3D + time) toolbox that includes all the
61 necessary computational steps for TFM. Experimentalists can input the raw microscopy images and follow
62 every computational step through interactive Graphical User Interfaces (GUIs) for parameter tuning. Users
63 can choose different image filters to process various types of data and use the Free Form Deformation
64 (FFD) algorithm for displacement measurement. In particular, FFD has proven to be superior to PIV and
65 has been used in various experimental studies involving 2D, 3D and 4D (time lapse) measurements in
66 single cell and multicellular systems [26]–[30]. Finally, accurate and computationally efficient force
67 calculation is provided by our recently published physically-based nonlinear inverse method (PBNIM) [31],
68 [32].

69 TFMLAB combines complex state of the art methods into a closed and user-friendly software that does
 70 not require code manipulations and allows for applying 4D TFM in biological studies holding strong
 71 promise for mechanobiology.

72

73 2. Software Description

74 2.1. Software Architecture

75 We developed TFMLAB in the MATLAB framework to provide robust and user-friendly processing of the
 76 microscopy data. The software has one main function main.m, which calls other routines at every step of
 77 computational TFM (see schematic in Fig 1). However, TFMLAB follows a “black box” fashion and the user
 78 only needs to interact with TFMLAB’s GUIs. Briefly, TFMLAB has the following steps: (1) microscopy image
 79 reading, (2) image processing, (3) displacement measurement and (4) force calculation. There is a GUI for
 80 parameter tuning before every step and result folders are stored between steps. While MATLAB
 81 orchestrates the workflow, some specific operations are performed by external software (see Table 1).

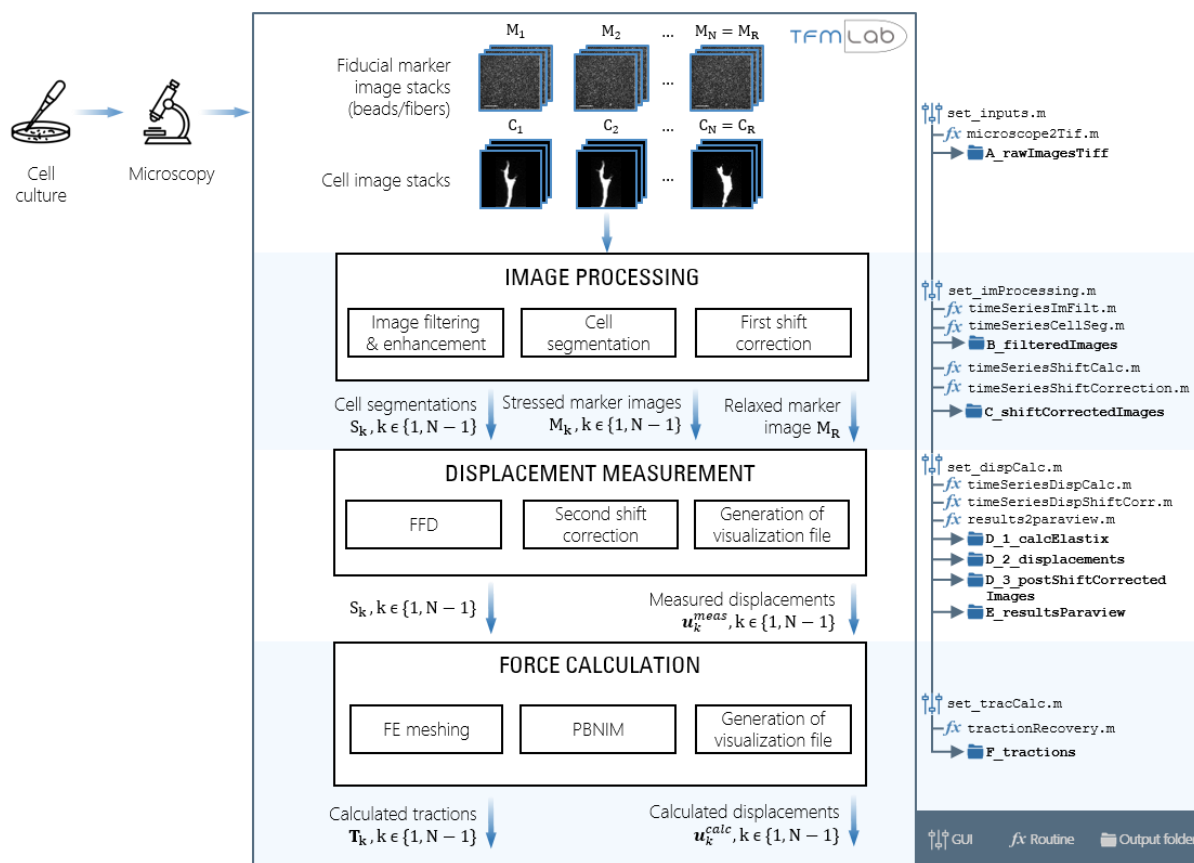


Fig 1. Basic flow chart of TFMLAB. After cell culture and microscopy imaging (left hand side), the user can input marker (M_k) and cell (C_k) image stacks into TFMLAB (top). The main steps of the workflow (middle), the GUI scripts, the name of the key MATLAB functions that perform the steps and the output folders that the software generates (right hand side) are shown. Briefly, after image processing, displacements (u_k^{meas}) in the marker images are measured by means of Free Form Deformation (FFD). These displacements and a finite element (FE) mesh of the cell and the hydrogel are used to calculate improved displacements u_k^{calc} and their associated tractions T_k , which fulfil the equilibrium of forces in the hydrogel with the Physically-Based Nonlinear Inverse Method (PBNIM). Icons used freely available from [50], [51].

82 *Table 1. External software used in TFMLAB. Please note that Abaqus and FreeFEM are two FE solver alternatives. Only one of them*
 83 *is necessary for force calculation.*

Software/toolbox	Freely available	Provided with TFMLAB	Use
Bioformats [33]	Yes	Yes	Microscopy image reading
DIPImage [34]	Yes	No	Image processing: image filtering and enhancement
Elastix [35]	Yes	Yes	Displacement measurement: FFD image registration
Paraview [36]	Yes	No	(Optional) results visualization
iso2mesh [37]	Yes	Yes	Force calculation: Automatic FE meshing
SuiteSparse [38]	Yes	Yes	Force calculation: PBNIM system of equations
Abaqus	No	No	Force calculation: FE solver
FreeFEM [39]	Yes	No	Force calculation: Alternative FE solver

84

85 2.2. Software Functionalities

86 The user must first run the script main.m in MATLAB and the steps depicted in Fig 1 follow, asking for user
 87 interaction through different GUIs.

88 *Microscopy image reading*

89 First, the user must provide input data. The GUI *set_inputs* will ask for an input microscopy file. For
 90 flexibility, TFMLAB uses the Bio-Formats toolbox which can read multiple microscopy file formats [33].
 91 From the input file, the software reads the channels corresponding to the cells (e.g., imaged after
 92 transduction with LifeAct for filamentous actin staining) and the fiduciary markers such as fluorescent
 93 beads and/or fibers (e.g., in case of a fibrillar collagen hydrogel imaged by means of second harmonic
 94 generation [27]). Any other channels (e.g. bright field, nuclei...) present in the microscopy file are ignored,
 95 as they are not necessary for TFM. The user can provide any number of images (time points) for a given
 96 sample as long as the field of view of the hydrogel remains constant. All the images are considered to
 97 conform different time points of the stressed state while the last image provided is considered to be the
 98 relaxed state. Function *microscope2Tif* then converts the input data into .tiff files. This is a standard
 99 format that maintains bit depth and is easy to access with any free software such as ImageJ. The data is
 100 split by channels (cell, beads and/or fibers) and time points (tp_01, tp_02,..., tp_R) and stored in the
 101 A_rawImagesTiff output folder.

102 *Image processing*

103 The GUI *set_imProcessing* allows the user to interactively tune image filtering and enhancement
 104 parameters. TFMLAB provides specific filters for cell, bead and fiber images, and tools for cell
 105 segmentation. There are multiple filtering options combining the MATLAB image processing toolbox and
 106 the DIPImage library [34] for versatility (see examples in section 3). The main function then calls the
 107 functions *timeSeriesImFilt* and *timeSeriesCellSeg* to process all the input images and stores them in the
 108 B_filteredImages output folder. Rigid image registration is done during the first shift correction step,
 109 correcting for any microscope stage related drifts. First, a phase correlation operation is done to calculate
 110 the shift between all the images and a reference image with the function *timeSeriesShiftCalc*. If only two

111 images are provided, the reference is the relaxed image. Otherwise, the reference is the middle time-
112 point. The bead/fiber images are used for this operation. Second, the function *timeSeriesShiftCorrection*
113 aligns the images from all the channels according to the calculated shift, and any non-overlapping image
114 borders are cropped such that all the images have equal size at the end of the operation. The resultant
115 images are stored in the C_shiftCorrectedImages output folder.

116 *Displacement measurement*

117 Displacement measurement is done by means of FFD-based image registration [26]. Briefly, a multivariate
118 B-spline function warps a moving image (a marker image at a certain time point of the stressed state, M_k)
119 to optimize the value of a distance metric that quantifies its similarity to a fixed image (the marker image
120 that represents the relaxed state, M_R). Using the GUI *set_dispCalc* the user can choose between different
121 optimizers, distance metrics and can tune the spacing between the control points of the B-spline curves
122 to adapt it to experimental conditions of each sample. The main function then calls *timeSeriesDispCalc*,
123 which uses the Elastix toolbox for efficient image registration as previously described [29], [30], [40]. The
124 cell segmentations S_k can be used as masks to ignore beads engulfed by the cells. The parameter and
125 performance files of the image registration are stored in output folder D_1_calcElastix. With a second
126 shift correction, the measured displacement fields $\mathbf{u}_k^{\text{meas}}$ are then corrected for any spurious rigid shifts
127 in *timeSeriesDispShiftCorr* and stored in folder D_2_displacements. This shift correction operation is done
128 by subtracting the mean from each displacement field component for the entire image stack. The images
129 (beads/fibers, cell and cell segmentations) are also corrected accordingly and stored in
130 D_3_postShiftCorrectedImages. Finally, function *results2paraview* generates .vtk files for vector field and
131 cell segmentation visualization in the free software Paraview [36] and stores them in folder
132 E_resultsParaview.

133 *Force calculation*

134 The user is asked to tune the force calculation parameters in GUI *set_tracCalc*. The cell segmentations
135 S_k are used to create a finite element (FE) mesh of the cell surface and the hydrogel domain with the open
136 source mesh generator iso2mesh [37]. The resultant 3D tetrahedral mesh is coarser away from the cell
137 surface. The GUI allows for tuning the element sizes and smoothening. Moreover, the user can define the
138 mechanical parameters of the hydrogel such as the elastic modulus or the Poisson's ratio (assuming linear
139 elastic, isotropic behavior). Since the displacement field $\mathbf{u}_k^{\text{meas}}$ is measured only at certain discrete
140 locations (beads/fibers), it is not error free and traction recovery is typically done by applying
141 regularization techniques to avoid overfitting. In TFMLAB, we used our novel PBNIM method which proved
142 to be more accurate than a non-regularized method on in silico and in vitro experiments [31], [32]. Briefly,
143 this method calculates a displacement field, $\mathbf{u}_k^{\text{calc}}$, that is minimally different from the measured one,
144 $\mathbf{u}_k^{\text{meas}}$, and that is enforced to fulfil equilibrium of forces in the hydrogel domain as a constraint (see details
145 in Appendix B). PBNIM was implemented in the function *tractionRecovery*. Since PBNIM is developed using
146 a FEM framework, a FE solver is required. TFMLAB is compatible with two FE solvers, namely, the
147 commercial Abaqus (Dassault Systemes Simulia Corporation, Providence, RI) and the open source
148 software FreeFEM [39]. Users can also pick between one of these FE solvers to compute tractions. Stiffness
149 matrices are computed through the selected FE solver. If Abaqus is selected, TFMLAB provides it with an

150 automatically written job file and the results are imported back into the MATLAB workspace in order to
151 preserve the “black box” architecture of TFMLAB. Similarly, TFMLAB automatically interacts with
152 FreeFEM, for which we developed specific FreeFEM routines. The minimization problem (Eq. B.3) is then
153 analytically derived turning into a system of equations solved by function *spqr_solve*, which is part of the
154 open source toolbox SuiteSparse [38]. This gives a displacement field $\mathbf{u}_k^{\text{calc}}$, which, unlike $\mathbf{u}_k^{\text{meas}}$, fulfils the
155 equilibrium of forces in the hydrogel domain. Following the Finite Element Method (FEM) procedure and
156 assuming a linear elastic behavior, stresses and tractions \mathbf{T}_k are forwardly obtained (Eq. B.4 - Eq. B.6).
157 Finally, .vtk files are generated for result visualization. All the results from this step are stored in the output
158 folder F_tractions.

159 *Output and other software features*

160 After computing the full workflow, the user might be interested in repeating a specific step with different
161 parameters while preserving the previous steps. GUIs allow for skipping steps starting from a specific step
162 of the workflow as opposed to running the entire workflow again. All the parameters selected by the user
163 are stored in .mat files for reproducibility. All the important output data (processed images, displacement
164 fields, force fields, etc) are stored in .mat and text files to allow for further analysis by the user. Together
165 with the .vtk visualization files, TFMLAB also stores a .psvm template for Paraview for automatic 3D vector
166 field rendering.

167 *2.3. Sample code snippets analysis (optional).*

168 **3. Illustrative Examples**

169 In this section, we present an example of the performance of TFMLAB using experimentally acquired data
170 from an in vitro model of angiogenesis in which Human Umbilical Vein Endothelial Cells (HUVECs) invade
171 a polyethylene glycol (PEG) hydrogel containing suspended 200nm fluorescent beads. More details on the
172 experimental protocol and microscopy imaging can be found in Appendix A.

173 For this example, we acquired cell and bead image stacks (290 x 290 x 45 μm) by means of confocal
174 microscopy before and after cell relaxation with Cytochalasin D (see Fig 2a-d and Supplementary Videos
175 1 and 2), with a voxel size of 0.57x0.57x0.5 μm^3 . An overview of the analysis of this data using TFMLAB is
176 provided in Supplementary Video 3. First, the bead images were processed by applying a Difference of
177 Gaussians (DoG) filter to enhance the spherical shape of the beads and noise removal, followed by a
178 contrast stretching operation (see Fig 2e-h). Next, the cell images were processed by applying a penalized
179 least squares-based denoising [41] and the cell body was segmented by applying Otsu thresholding and
180 by removing small binary objects (see Fig 2i-k). Finally, shifts caused by the microscope stage were
181 removed by applying phase-correlation-based rigid image registration (see Fig 2l-o). Before shift
182 correction, a distinct shift that affects all the beads of the image is present (Fig 2l, n). After shift correction,
183 the only bead movements remaining happen around the sprout, indicating cell-matrix interactions (Fig
184 2m, o).

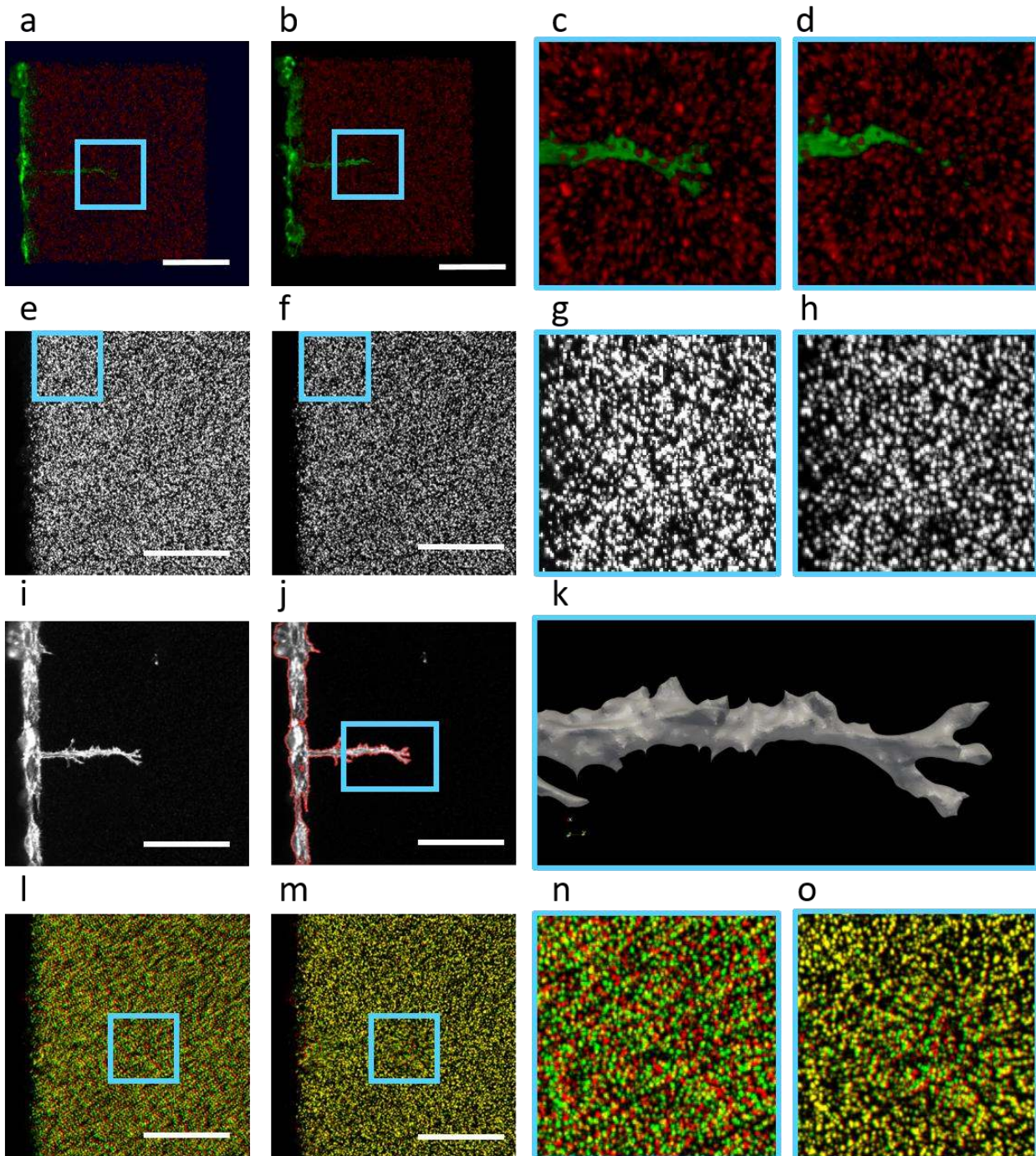


Fig 2. Image processing steps in TFMLAB. (a,b) 3D renders of the stressed and relaxed images as obtained by means of confocal microscopy (cell channel in green, beads channel in red). (c,d) Zoomed in regions from the raw stressed and relaxed images. (e,f) Maximum projections of a bead image before and after image filtering and enhancement. (g,h) Zoomed in regions before and after enhancement. (i) Maximum intensity projection of the raw cell image. (j) Maximum intensity projection of the filtered cell image and segmentation boundary (red). (k) 3D render (Paraview) of the resultant cell segmentation. (l,m) Maximum intensity projection overlay of the stressed (green) and relaxed (red) bead images before and after shift correction. (n,o) Zoomed in regions before and after shift correction. Scale bars: 100 μ m.

185 After image processing, non-rigid displacements are measured by FFD and the PBNIM method is applied
186 to recover cellular forces. Fig 3a shows TFMLAB's force recovery GUI *set_tracCalc*. The cell surface can be

187 further smoothed prior to FE meshing to ease the meshing process. The user can tune and visualize the
188 resultant FE mesh before computing forces. For this example, the resultant FE mesh had ~ 90000 4-node
189 3-D linear tetrahedral elements. The elastic modulus was set to 200Pa based on experimental results and
190 the Poisson's ratio was assumed to be 0.2. Table 2 shows the computational times to complete every step
191 in TFMLAB on an Intel Core i7-7700 CPU 3.60GHz with a Windows operating system and 16 GB of RAM.
192 These numbers exclude the time invested in parameter tuning, which for an experienced user can be
193 around 10 minutes with the majority of this time spent on image filtering, cell segmentation and FE
194 meshing.

195 Results show a clear pulling pattern near the sprout tip inducing up to $\sim 6\mu\text{m}$ matrix displacements (see
196 Fig 3b). The recovered tractions present maxima at the tips of the cell's protrusion of around 150Pa (see
197 Fig 3c). While this displacement field pattern around angiogenic sprouts has been reported in previous
198 studies [30], [42]–[44], TFMLAB additionally incorporates quantification of traction magnitude and
199 direction. This can be a crucial tool for the quantification of cell mechanical behavior in 3D, ECM-mimicking

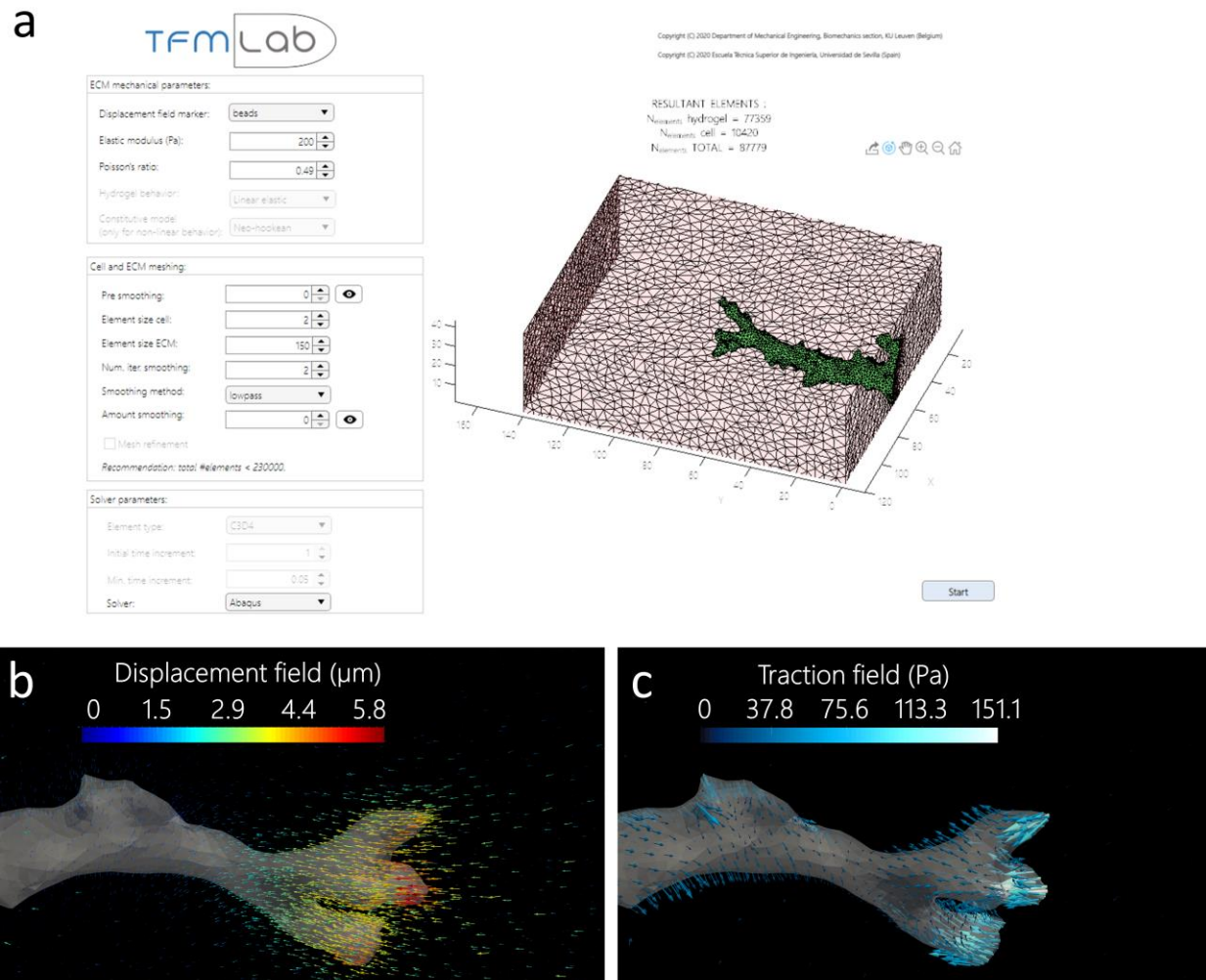


Fig 3. (a) GUI for FE meshing and force calculation. (b) 3D render (Paraview) of the 3D displacement field (arrows) around the sprout tip as calculated by PBNIM. (c) 3D render (Paraview) of the traction field (arrows) around the tip of the sprout as calculated by PBNIM.

200 hydrogels, both for single cells as well as multicellular structures and for applications such as disease
201 modeling, regenerative medicine and tissue engineering as well as developmental biology. Further
202 advantages of TFMLAB are discussed in section 4.

203 *Table 2. Computational times for every step of TFMLAB for the given example (one time point of a TFM experiment).*

TFMLAB step	Computational time (seconds)
Image filtering	25.71
Shift calculation	2.33
Pre-shift correction	19.72
Cell segmentation	9.86
Displacement measurement	63.43
Post-shift correction	31.71
Force calculation	56.15
TOTAL (minutes)	3.48

204

205 **4. Impact**

206 With this work, we provide an easy-to-use and versatile open source code to perform 4D TFM, making
207 advanced cell mechanical data accessible to researchers with various (including limited) technical
208 backgrounds. To our knowledge, the following features make TFMLAB an unprecedented tool in the field
209 of mechanobiology:

- 210 • It is an “all in one” software. Currently, a typical researcher running computational 3D TFM uses
211 e.g. ImageJ for image processing and extra software for displacement and force calculation. This
212 leads to time-consuming work adapting input data to ensure compatibility between software. In
213 contrast, researchers have all the tools they need in TFMLAB.
- 214 • It includes state of the art methods of proven usefulness in multiple TFM studies [26]–[32].
- 215 • While TFMLAB is a “black box” software, its GUIs especially offer ease of usability for researchers
216 with limited programming experience and enable viewing progress of the various steps and
217 parameter tuning.
- 218 • TFMLAB does not require having any commercial software other than MATLAB. As other state of
219 the art TFM software [19], [21], [45], TFMLAB is compatible with Abaqus, a sophisticated and
220 technical FE solver. However, it also offers an open source alternative, namely FreeFEM.
221 Moreover, the user needs little knowledge on FE modelling as only basic parameter tuning (via a
222 TFMLAB GUI) is required.
- 223 • It is versatile as it can handle different 3D TFM approaches. Current research includes both bead-
224 based TFM [20], [46], [47] and fiber-based TFM (with fiber networks e.g. being imaged by means
225 of label-free techniques such as second harmonic generation or confocal reflection microscopy)
226 [23], [27], [48]. Our software includes specific image filters for both markers and the FFD algorithm
227 handles both of them [27], [30]. Furthermore, a user can run a classical TFM problem (using a
228 stressed image and a relaxed image, as in the example in section 3) or time-lapse TFM (using a
229 sequence of stressed images and one relaxed image). If the researcher’s experimental protocol

230 does not include cell imaging, displacement calculation based on the fiducial markers is still
231 possible.

232 The compactness, user-friendliness and versatility of our toolbox makes it usable in studying many
233 physiological or pathological processes where cell-matrix mechanics play an important role. Such a tool
234 can become key in unravelling cell mechanical time-dependant interactions with their 3D
235 microenvironment, aspects at the forefront of recent mechanobiological research [25], [30], [48], [49].

236 **5. Conclusions**

237 TFMLAB is an open-source MATLAB toolbox that seeks to bring 4D TFM closer to medical and biological
238 researchers that do not necessarily have a strong technical background, thereby facilitating the transition
239 of TFM technology from (biomedical) engineering – and/or (bio-)physics-dominated research
240 environments towards medicine and biology. All the necessary steps for computing 4D cellular forces are
241 included in one easy-to-use package (microscopy image reading and processing, displacement
242 measurement, force recovery and visualization file generation). We demonstrated the usefulness and
243 efficiency of the software in an example using real experimental data. We expect that researchers will
244 find TFMLAB useful independent of their programming or technical background.

245 **Conflict of Interest**

246 No conflict of interest exists:

247 We wish to confirm that there are no known conflicts of interest associated with this publication and there
248 has been no significant financial support for this work that could have influenced its outcome.

249

250 **Acknowledgements**

251 The authors thank Dr Marie-Mo Vaeyens, Dr Mar Córdor and Janne de Jong for their valuable code testing
252 and feedback. The authors also thank the Ranga lab for providing the PEG precursors used in hydrogel
253 preparation. J.B.F. was supported by the Research Foundation Flanders (FWO) (travel grant for a long stay
254 abroad, FWO grant V413019N). J.B.F. and H.V.O. were supported by KU Leuven internal funding
255 C14/17/111. A.S. was supported by the FWO SB grant 1S68818N. M. B. was supported by the FWO project
256 G085018N and the Prosperos project, funded by the Interreg VA Flanders – The Netherlands program, CCI
257 grant no. 2014TC16RFCB046. J.A.S.H. was supported by the José Castillejo fellowship of the Ministerio de
258 Educación, Cultura y Deporte of Spain, grant number CAS17/00096 and Spanish Ministry of Economy and
259 Competitiveness (MINECO) through the project PGC2018-097257-B-C31. H.V.O. was supported by the
260 European Research Council under the European Union's Seventh Framework Program (FP7/2007–
261 2013)/ERC Grant Agreement No. 308223), by an FWO grant (G087018N) and by an FWO / Hercules
262 infrastructure grant (G0H6316N). The financial support is gratefully acknowledged.

263

264

265 **References**

- 266 [1] C. M. Kraning-Rush, J. P. Califano, and C. A. Reinhart-King, "Cellular traction stresses increase
267 with increasing metastatic potential," *PLoS One*, vol. 7, no. 2, Feb. 2012.
- 268 [2] K. A. Jansen, R. G. Bacabac, I. K. Piechocka, and G. H. Koenderink, "Cells actively stiffen fibrin
269 networks by generating contractile stress," *Biophys. J.*, vol. 105, no. 10, pp. 2240–2251, Nov.

- 270 2013.
- 271 [3] U. S. Schwarz and J. R. D. Soiné, “Traction force microscopy on soft elastic substrates: A guide
272 to recent computational advances,” *Biochim. Biophys. Acta - Mol. Cell Res.*, vol. 1853, no. 11,
273 pp. 3095–3104, 2015.
- 274 [4] M. L. Kutys and C. S. Chen, “Forces and mechanotransduction in 3D vascular biology,” *Current
275 Opinion in Cell Biology*, vol. 42. Elsevier Ltd, pp. 73–79, 01-Oct-2016.
- 276 [5] J. A. Mulligan, F. Bordeleau, C. A. Reinhart-King, and S. G. Adie, “Measurement of dynamic cell-
277 induced 3D displacement fields in vitro for traction force optical coherence microscopy,”
278 *Biomed. Opt. Express*, vol. 8, no. 2, p. 1152, Feb. 2017.
- 279 [6] W. J. Polacheck and C. S. Chen, “Measuring cell-generated forces: A guide to the available
280 tools,” *Nature Methods*, vol. 13, no. 5. Nature Publishing Group, pp. 415–423, 01-May-2016.
- 281 [7] M. Dembo and Y.-L. Wang, “Stresses at the Cell-to-Substrate Interface during Locomotion of
282 Fibroblasts,” *Biophys. J.*, vol. 76, no. 4, pp. 2307–2316, 1999.
- 283 [8] N. Q. Balaban *et al.*, “Force and focal adhesion assembly: A close relationship studied using
284 elastic micropatterned substrates,” *Nat. Cell Biol.*, vol. 3, no. 5, pp. 466–472, Apr. 2001.
- 285 [9] A. J. Engler, S. Sen, H. L. Sweeney, and D. E. Discher, “Matrix Elasticity Directs Stem Cell
286 Lineage Specification,” *Cell*, vol. 126, no. 4, pp. 677–689, Aug. 2006.
- 287 [10] Nobuhito Mori, “FrontPage - mpiv - MATLAB PIV Toolbox.” [Online]. Available:
288 <http://www.oceanwave.jp/software/mpiv/>. [Accessed: 07-Apr-2020].
- 289 [11] D. Blair and E. Dufresne, “Matlab Particle Tracking.” [Online]. Available:
290 <http://site.physics.georgetown.edu/matlab/>. [Accessed: 07-Apr-2020].
- 291 [12] P. C. Hansen, “regtools - File Exchange - MATLAB Central.” [Online]. Available:
292 <https://www.mathworks.com/matlabcentral/fileexchange/52-regtools>. [Accessed: 07-Apr-
293 2020].
- 294 [13] Q. Tseng, “Traction Force Microscopy - ImageJ plugins.” [Online]. Available:
295 <https://sites.google.com/site/qingzongtseng/tfm>. [Accessed: 07-Apr-2020].
- 296 [14] The Franck Lab, “DOWNLOADS | francklaboratory.” [Online]. Available:
297 <https://www.franck.engin.brown.edu/downloads>. [Accessed: 07-Apr-2020].
- 298 [15] R. W. Style *et al.*, “Traction force microscopy in physics and biology,” *Soft Matter*, vol. 10, no.
299 23. Royal Society of Chemistry, pp. 4047–4055, 21-Jun-2014.
- 300 [16] Y. Huang, G. Gommer, and B. Sabass, “A Bayesian traction force microscopy method with
301 automated denoising in a user-friendly software package,” *Comput. Phys. Commun.*, p.
302 107313, Apr. 2020.
- 303 [17] S. J. Han, Y. Oak, A. Groisman, and G. Danuser, “Traction microscopy to identify force
304 modulation in subresolution adhesions,” *Nat. Methods*, vol. 12, no. 7, pp. 653–656, Jul. 2015.
- 305 [18] D. Song, N. Hugenberg, and A. A. Oberai, “Three-dimensional traction microscopy with a
306 fiber-based constitutive model,” *Comput. Methods Appl. Mech. Eng.*, vol. 357, p. 112579, Dec.
307 2019.
- 308 [19] W. R. Legant, J. S. Miller, B. L. Blakely, D. M. Cohen, G. M. Genin, and C. S. Chen, “Measurement
309 of mechanical tractions exerted by cells in three-dimensional matrices,” *Nat. Methods*, vol. 7,
310 no. 12, pp. 969–971, Dec. 2010.
- 311 [20] N. Gjorevski, A. S. Piotrowski, V. D. Varner, and C. M. Nelson, “Dynamic tensile forces drive
312 collective cell migration through three-dimensional extracellular matrices,” *Sci. Rep.*, vol. 5, p.
313 11458, Jul. 2015.
- 314 [21] M. Córdor and J. M. García-Aznar, “An iterative finite element-based method for solving
315 inverse problems in traction force microscopy,” *Comput. Methods Programs Biomed.*, vol. 182,
316 p. 105056, Dec. 2019.
- 317 [22] E. Lejeune, A. Khang, J. Sansom, and M. S. Sacks, “FM-Track: A fiducial marker tracking
318 software for studying cell mechanics in a three-dimensional environment,” *SoftwareX*, vol.
319 11, 2020.

- 320 [23] J. Steinwachs *et al.*, “Three-dimensional force microscopy of cells in biopolymer networks,”
321 *Nat. Methods*, vol. 13, no. 2, pp. 171–176, 2016.
- 322 [24] M. C ndor, J. Steinwachs, C. Mark, J. M. Garc a-Aznar, and B. Fabry, “Traction Force
323 Microscopy in 3-Dimensional Extracellular Matrix Networks,” in *Current Protocols in Cell*
324 *Biology*, vol. 75, no. 1, Hoboken, NJ, USA: John Wiley & Sons, Inc., 2017, pp. 10.22.1-10.22.20.
- 325 [25] C. Mark *et al.*, “Collective forces of tumor spheroids in three-dimensional biopolymer
326 networks,” *Elife*, vol. 9, Apr. 2020.
- 327 [26] A. Jorge-Pe nas *et al.*, “Free form deformation-based image registration improves accuracy of
328 traction force microscopy,” *PLoS One*, vol. 10, no. 12, pp. 1–22, 2015.
- 329 [27] A. Jorge-Pe nas *et al.*, “3D full-field quantification of cell-induced large deformations in
330 fibrillar biomaterials by combining non-rigid image registration with label-free second
331 harmonic generation,” *Biomaterials*, vol. 136, pp. 86–97, Aug. 2017.
- 332 [28] A. Izquierdo- lvarez, D. A. Vargas,  . Jorge-Pe nas, R. Subramani, M.-M. Vaeyens, and H. Van
333 Oosterwyck, “Spatiotemporal Analyses of Cellular Traction Describe Subcellular Effect of
334 Substrate Stiffness and Coating,” *Ann. Biomed. Eng.*, vol. 47, no. 2, pp. 624–637, Feb. 2019.
- 335 [29] C. Steuwe *et al.*, “Fast quantitative time lapse displacement imaging of endothelial cell
336 invasion,” *PLoS One*, vol. 15, no. 1, p. e0227286, Jan. 2020.
- 337 [30] M.-M. Vaeyens *et al.*, “Matrix deformations around angiogenic sprouts correlate to sprout
338 dynamics and suggest pulling activity,” *Angiogenesis*, Jan. 2020.
- 339 [31] J. A. Sanz-Herrera, J. Barrasa Fano, M. C ndor, and H. Van Oosterwyck, “Inverse method
340 based on 3D nonlinear physically constrained minimisation in the framework of traction
341 force microscopy,” *Soft Matter*, 2020.
- 342 [32] J. Barrasa-Fano, A. Shapeti, J. De Jong, A. Ranga, J. A. Sanz-Herrera, and H. Van Oosterwyck,
343 “Advanced in silico validation framework for three-dimensional Traction Force Microscopy
344 and application to an in vitro model of sprouting angiogenesis,” *bioRxiv*, p.
345 2020.12.08.411603, Dec. 2020.
- 346 [33] M. Linkert *et al.*, “Metadata matters: Access to image data in the real world,” *Journal of Cell*
347 *Biology*, vol. 189, no. 5. The Rockefeller University Press, pp. 777–782, 31-May-2010.
- 348 [34] “DIPimage - DIPimage & DIPlib.” [Online]. Available: <http://www.diplib.org/dipimage>.
349 [Accessed: 04-May-2020].
- 350 [35] S. Klein, M. Staring, K. Murphy, M. A. Viergever, and J. P. W. Pluim, “Elastix: A toolbox for
351 intensity-based medical image registration,” *IEEE Trans. Med. Imaging*, vol. 29, no. 1, pp.
352 196–205, Jan. 2010.
- 353 [36] U. Ayachit, *The ParaView Guide: A Parallel Visualization Application*. Kitware, 2015.
- 354 [37] Qianqian Fang and D. A. Boas, “Tetrahedral mesh generation from volumetric binary and
355 grayscale images,” in *2009 IEEE International Symposium on Biomedical Imaging: From Nano*
356 *to Macro*, 2009, pp. 1142–1145.
- 357 [38] T. A. Davis, “Algorithm 915, SuiteSparseQR: Multifrontal multithreaded rank-revealing
358 sparse QR factorization,” *ACM Trans. Math. Softw.*, vol. 38, no. 1, pp. 1–22, Nov. 2011.
- 359 [39] F. Hecht, “New development in freefem+,” *J. Numer. Math.*, vol. 20, no. 3–4, pp. 251–265, Dec.
360 2012.
- 361 [40] A. Jorge-Pe nas, A. Mu oz-Barrutia, E. M. De-Juan-Pardo, and C. Ortiz-De-Solorzano,
362 “Validation tool for traction force microscopy,” *Comput. Methods Biomech. Biomed. Engin.*,
363 vol. 18, pp. 1377–1385, 2015.
- 364 [41] D. Garcia, “Robust smoothing of gridded data in one and higher dimensions with missing
365 values,” *Comput. Stat. Data Anal.*, vol. 54, no. 4, pp. 1167–1178, Apr. 2010.
- 366 [42] Y. Du, S. C. B. Herath, Q. Wang, D. Wang, H. H. Asada, and P. C. Y. Chen, “Three-Dimensional
367 Characterization of Mechanical Interactions between Endothelial Cells and Extracellular
368 Matrix during Angiogenic Sprouting,” *Sci. Rep.*, vol. 6, no. 1, p. 21362, Aug. 2016.
- 369 [43] C. Yoon *et al.*, “Myosin IIA-mediated forces regulate multicellular integrity during vascular

- 370 sprouting," *Mol. Biol. Cell*, vol. 30, no. 16, pp. 1974–1984, Jul. 2019.
- 371 [44] Y. Du, S. C. B. Herath, Q. G. Wang, H. Asada, and P. C. Y. Chen, "Determination of Green's
372 function for three-dimensional traction force reconstruction based on geometry and
373 boundary conditions of cell culture matrices," *Acta Biomater.*, vol. 67, pp. 215–228, Feb.
374 2018.
- 375 [45] J. Toyjanova *et al.*, "3D Viscoelastic traction force microscopy," *Soft Matter*, vol. 10, no. 40, pp.
376 8095–8106, Aug. 2014.
- 377 [46] J. A. Mulligan, X. Feng, and S. G. Adie, "Quantitative reconstruction of time-varying 3D cell
378 forces with traction force optical coherence microscopy," *Sci. Rep.*, vol. 9, no. 1, Dec. 2019.
- 379 [47] L. Dong and A. A. Oberai, "Recovery of cellular traction in three-dimensional nonlinear
380 hyperelastic matrices," *Comput. Methods Appl. Mech. Eng.*, vol. 314, pp. 296–313, Feb. 2017.
- 381 [48] D. Shakiba *et al.*, "The Balance between Actomyosin Contractility and Microtubule
382 Polymerization Regulates Hierarchical Protrusions That Govern Efficient Fibroblast-
383 Collagen Interactions," *ACS Nano*, Apr. 2020.
- 384 [49] M. Córdor *et al.*, "Breast Cancer Cells Adapt Contractile Forces to Overcome Steric
385 Hindrance," *Biophys. J.*, vol. 116, no. 7, pp. 1305–1312, Apr. 2019.
- 386 [50] "agus raharjo on Iconfinder." [Online]. Available: <https://www.iconfinder.com/agusraharj>.
387 [Accessed: 20-Oct-2020].
- 388 [51] "Minimal disease icons by PictureWindow." [Online]. Available:
389 <https://www.iconfinder.com/iconsets/minimal-disease>. [Accessed: 20-Oct-2020].
- 390

391 **Appendices**

392

393 **A. Experimental protocol**

394 Commercially available pooled wild type human umbilical vein endothelial cells (HUVEC, Angio-
395 Proteomie) were cultured in complete endothelial growth medium (EGM-2, Lonza) and used at passage
396 4. HUVECs were transduced with adenoviral LifeAct-GFP2 (Ibidi) on the day before hydrogel preparation.
397 Enzymatically crosslinked poly-ethylene glycol (PEG) hydrogels comprised of an MMP-sensitive peptide
398 modified PEG precursor (8-arm 40kDa), Lys-RGD peptide (Pepmic), and 0.1 μM Sphingosine-1-Phosphate
399 (Sigma-Aldrich) were suspended with 0.2 μm red fluorescent carboxylated polystyrene microspheres
400 (ThermoFischer). PEG solution was pipetted into a previously described [30] imaging chamber attached
401 to the glass bottom of a petri dish, and further allowed to crosslink for 30 min at room temperature. A
402 confluent cell monolayer was then achieved by seeding 50,000 LifeAct transduced HUVECs per gel and
403 incubating the dishes vertically at 37°C, 5% CO₂ to allow cell adhesion onto the PEG meniscus. Finally,
404 EGM-2 was added and dishes were placed horizontally at standard conditions in the incubator for 16h
405 before experimentation.

406 Sprouts invading the PEG hydrogel were imaged using a Leica SP8 inverted confocal microscope with a
407 25x0.95 NA water-immersion objective to obtain image stacks of 290 x 290 x 45 μm at 0.5 μm z-spacing.
408 The green fluorescent cell channel and the red fluorescent beads channel were simultaneously imaged to
409 obtain two sets of images; first when the beads are in a stressed state and the cells are contractile, and
410 the second when the beads are in a relaxed state and the cells are non-contractile. The stressed state was
411 imaged immediately after placing the dish upon the stage and locating the sprout of interest. The relaxed
412 state was then induced by treating the cells with Cytochalasin D (dissolved in DMSO, Sigma Aldrich) at 4
413 μM for 50 minutes followed by image acquisition in the same location.

414 **B. Traction recovery by means of PBNIM**

415 PBNIM was first developed in the context of nonlinear elasticity. A detailed description of the numerical
416 implementation of this method is provided in [31]. TFMLAB uses an adapted implementation for linear
417 elasticity, as described in our preprint [32]. Briefly, this method calculates a displacement field, \mathbf{u}^{calc} , that
418 is minimally different from the measured one, \mathbf{u}^{meas} , and that is enforced to fulfil equilibrium of forces in
419 the hydrogel domain as a constraint. This can be mathematically written as follows,

$$\min_{\mathbf{u}_c^{\text{calc}}, \mathbf{u}_h^{\text{calc}}} \left\| \frac{1}{2} (\mathbf{u}_c^{\text{calc}} - \mathbf{u}_c^{\text{meas}})^2 + \frac{1}{2} (\mathbf{u}_h^{\text{calc}} - \mathbf{u}_h^{\text{meas}})^2 \right\| \quad \text{Eq. B.1}$$

s. t.
 $\mathbf{F}_h = 0$

420

421 where \mathbf{F} is the nodal reaction forces vector which accounts for external or internal prescribed forces or
422 displacements and c and h denote the cell boundary domain and the hydrogel domain, respectively. Using
423 a FEM framework and including the equilibrium constraint as a Langrange multiplier, Eq. B.1 can be
424 rewritten as,

425

$$\min_{\mathbf{u}_c^{\text{calc}}, \mathbf{u}_h^{\text{calc}}} \left\| \frac{1}{2} (\mathbf{u}_c^{\text{calc}} - \mathbf{u}_c^{\text{meas}})^2 + \frac{1}{2} (\mathbf{u}_h^{\text{calc}} - \mathbf{u}_h^{\text{meas}})^2 + \Theta \cdot \eta \right\| \quad \text{Eq. B.2}$$

426 where Θ is the equilibrium constraint equation and η is the Lagrange multiplier. The minimum of Eq. B.2
 427 can be calculated analytically and rewritten in matrix form as (the details or the formulation are given in
 428 [32]),

$$\begin{bmatrix} \mathbf{I} & 0 & \mathbf{K}_{\text{ch}} \\ 0 & \mathbf{I} & \mathbf{K}_{\text{hh}} \\ \mathbf{K}_{\text{hc}} & \mathbf{K}_{\text{hh}} & 0 \end{bmatrix} \cdot \begin{bmatrix} \mathbf{u}_c^{\text{calc}} \\ \mathbf{u}_h^{\text{calc}} \\ \eta \end{bmatrix} = \begin{bmatrix} \mathbf{u}_c^{\text{meas}} \\ \mathbf{u}_h^{\text{meas}} \\ 0 \end{bmatrix} \quad \text{Eq. B.3}$$

429 where \mathbf{K}_{hc} , \mathbf{K}_{ch} and \mathbf{K}_{hh} are the parts of the stiffness matrix associated with the two domains c and h.

430 Next, the strain field at each Gauss point of an element (e) is computed as,

$$\boldsymbol{\varepsilon}^{(e)} = \mathbf{B} \cdot \mathbf{u}^{\text{calc}(e)} \quad \text{Eq. B.4}$$

431 where \mathbf{B} is the gradient matrix of the shape functions. The stress tensor is calculated at each Gauss point
 432 of an element (e) based on the linear elastic, isotropic and homogeneous constitutive properties as,

$$\boldsymbol{\sigma}^{(e)} = 2\mu \cdot \boldsymbol{\varepsilon}^{(e)} + \lambda \cdot \text{tr}(\boldsymbol{\varepsilon}^{(e)})\mathbf{I} \quad \text{Eq. B.5}$$

433 where μ and λ are the Lamé constants of the hydrogel. $\boldsymbol{\sigma}^{(e)}$ is then averaged from Gauss points to the
 434 nodes i of the FE mesh. Traction vectors are computed at the cell boundary domain using the Cauchy relation,

$$\mathbf{T}_i = \boldsymbol{\sigma}_i \cdot \mathbf{n}_i \quad \text{Eq. B.6}$$

435 where \mathbf{T}_i is the traction vector at the nodes i of the FE mesh and \mathbf{n}_i is the outward normal to node i.

436

437 **Required Metadata**

438

439 **Current code version**

440 *Ancillary data table required for subversion of the codebase. Kindly replace examples in right column with the*
441 *correct information about your current code, and leave the left column as it is.*

442

443 *Table 1 – Code metadata (mandatory)*

Nr	Code metadata description	Please fill in this column
C1	Current code version	<i>v1.0</i>
C2	Permanent link to code/repository used of this code version	https://gitlab.kuleuven.be/MATRIX/Jorge/tfmlab_public
C3	Legal Code License	<i>LGPL v3.0</i>
C4	Code versioning system used	<i>Gitlab</i>
C5	Software code languages, tools, and services used	<i>MATLAB</i>
C6	Compilation requirements, operating environments & dependencies	<i>Image processing toolbox, signal processing toolbox (MATLAB), DIPImage library, Elastix</i>
C7	If available Link to developer documentation/manual	https://gitlab.kuleuven.be/MATRIX/Jorge/tfmlab_public/-/blob/public_tfmlab/manual.pdf
C8	Support email for questions	<i>jorge.barrasafano@kuleuven.be</i>

444